Optical Diagnostics for the Study of Plasma Evolution in Linear Theta-Pinch TC-1

M. Machida, S.V. Lebedev*, S. A. Moshkalyov†, D. O. Campos, L. A. Berni

Instituto de Física "Gleb Wataghin", Universidade Estadual de Campinas, C.P. 6165, 13083-970, Campinas, S.P., Brazil

Received July 15, 1996

The plasma generated in the field reversed theta-pinch TC-1 discharge was investigated by means of a number of optical diagnostics: CO_2 laser-based interferometry, visible-VUV spectroscopy and ruby laser Thomson scattering. The evolution of the local electron density was studied by CO_2 laser intereferometry. Thomson scattering was employed for measurements of the electron density and temperature with high spatial resolution. The temporal behavior of line emission of oxygen and carbon in various ionization stages was studied by VUV spectroscopy. The time dependence of the electron temperature was evaluated from the analysis of the time history of line emission of impurity ions. The ion temperature was measured from the Doppler-broadened oxygen line emission profiles.

I. Introduction

The TC-1 device[1] is a linear field reversed theta-pinch[2] operating at the Plasma Laboratory at UNICAMP. The lay-out of the device and the diagnostic system used in the experiments is depicted in the Fig. 1. The magnetic configuration is formed with a solenoid coil of 16 cm internal diameter and two mirror coils of 10 cm length and 15 cm internal diameter. Total length of the device is 65 cm. Vacuum chamber is a Pyrex tube of 14.5 cm diameter which is pumped out with a diffusion pump. Before a discharge the chamber is filled with H_2 at 0.5 - 5 mTorr pressure. Preionization of the gas is provided by a continuous inductively coupled RF discharge (30 MHz, 100 W). A set of capacitor banks is used as power supply for the magnetic system. The electrical scheme of the device is shown in the Fig. 2 and the typical discharge current sequence is shown in the Fig. 3. The amplitude of the magnetic field was 3.5 kG and the experiments have been performed in the regimes both with and without crowbar. When crowbar was not used, evolution of the plasma parameters was studied only around the first maximum of the magnetic field.

For the investigation of plasma evolution during the discharge a number of optical diagnostic techniques have been developed: ruby laser-based Thomson scattering for the measurements of plasma density and temperature with high spatial resolution, CO_2 laser-based interferometry (wavelength 10.6 μm) for the line-of-sight integrated measurements of plasma density temporal evolution, optical spectroscopy in the vacuum ultraviolet (VUV) , UV and visible spectral ranges for the study of time behavior of hydrogen and impurities line emission, as well as for the monitoring of the continuum emission from plasma. A detailed description of the Thomson scattering diagnostic, including the performance of a new multi-pass system of laser probing is given elsewhere[3,4]. The results of the study of the spectral resolution, available with a VUV spectrometer, employed in the experiments, have been reported in Ref. [5]. In this paper the combined use of the CO_2 interferometer and VUV-visible spectroscopy techniques for the investigation of a fast theta-pinch plasma discharge is described in more detail.

*On leave from Budker Institute of Nuclear Physics-Novosibirsk, Russia

†On leave from State Tech. University - St. Petersburg, Russia.

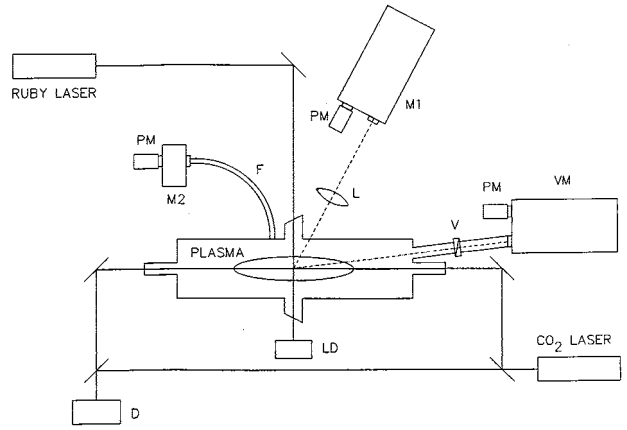

Figure 1: Schematic of the field-reversed theta-pinch TC-1 and the diagnostic system used in experiments. M1 and M2 - monochromators, VM - vacuum monochromator, V - vacuum valve, PM - photomultipliers, LD- light dump and L - lense optical system of light collection for Thomson scattering, F-optical fiber, D-infrared detector for CO_2 laser interferometry.

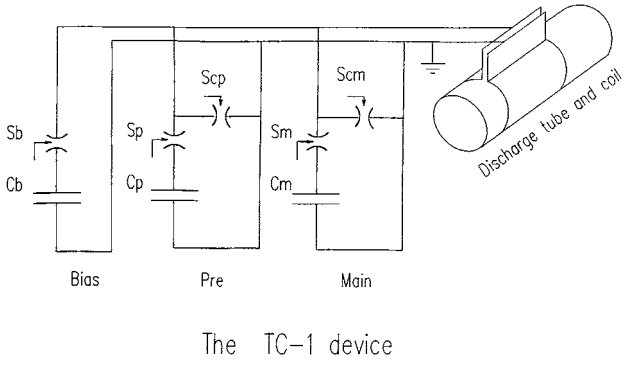

Figure 2: Electrical scheme of the TC-1 device.

II. Experimental techniques

II.1. CO_2 laser interferometer

To study the plasma density evolution a CO_2-laser based interferometer has been developed. The schematic of the diagnostic is presented in Fig. 4. A 5 W CO_2 laser is used as a source of radiation. The laser beam is splitted at the beamsplitter BS1 and the probing beam passes through the plasma in axial or side-on direction. Alignment of the interferometer is provided by a He-Ne laser beam superposed on the CO_2 laser beam at the ZnSe beamsplitter BS1. The probing and the reference beams are mixed at the beamsplitter BS2 and a liquid nitrogen-cooled HgCdTe photoconductive detector is used to measure the interference signal. The interferometer was aligned to obtain an interference fringe size larger than the size of the sensitive area of the detector (2 x 2 mm). For the amplitude calibration of the interference signal an oscillating mirror in the reference path of interferometer was installed. The frequency of interference fringes due to the mirror movement is up to 0.3 MHz. Before the discharge the interferometer signal is determined only by the mirror movement, so the amplitude A and the modulation frequency ω may be determined from this part of the signal. The signal during the discharge is given by

$$S = A \cdot \cos(\omega \cdot t + \varphi(t)) \qquad (1)$$

The phase shift φ due to the plasma is calculated as

$$\varphi(t) = arcos\left(\frac{S}{A}\right) - \omega \cdot t \ . \qquad (2)$$

This approach allows to eliminate the effect of absorption and refraction of the probing laser beam on the results of measurements. Mechanical vibrations had a minimal characteristic period much larger than the observation time of interest ($\sim$50 μs), and therefore did not influence the measurements. For the experiments under consideration we can neglect the plasma gyrofrequency and electron collision rate, in comparison with laser frequency. The line plasma density then is given by a well-known formula

$$\varphi = \pi/(\lambda n_{cr}) \int n_e dl \ . \qquad (3)$$

For the case of CO_2 laser ($\lambda = 10.6\mu$ m), $\varphi = 2\pi \cdot 4.75 \cdot 10^{-17} \cdot \int n_e \ dl$, where φ is in radians and line plasma density $\int n_e dl$ is in cm^{-2}. As a result, an expected phase shift for typical plasma parameters of TC-1 ($n_e \sim 3.10^{15}$ cm^{-3}, length 60 cm and diameter 5 cm) is about 8 fringes for longitudinal probing and about 1 fringe for side-on measurements.

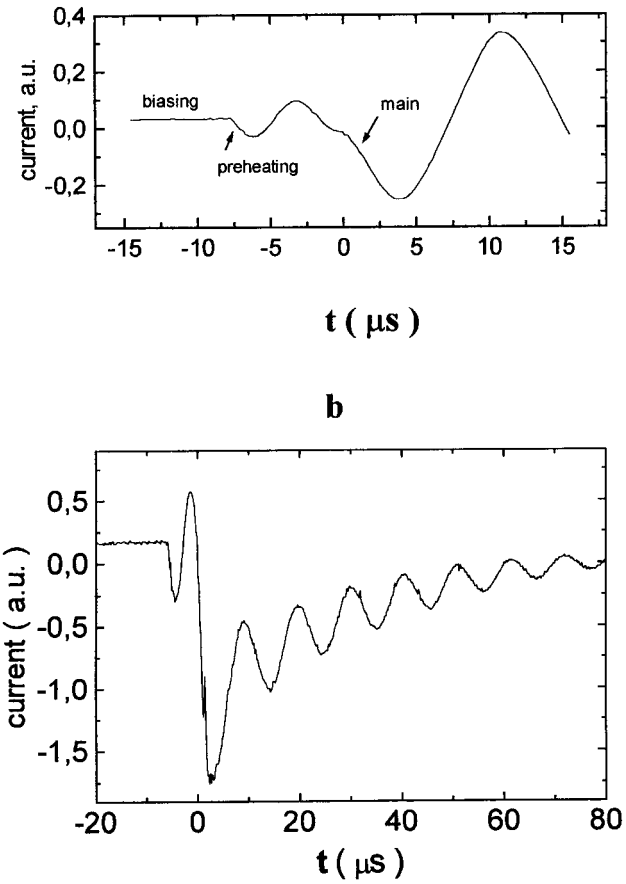

Figure 3: Magnetic field waveforms of the TC-1 device in the regimes without crowbar (a) and with crowbar (b).

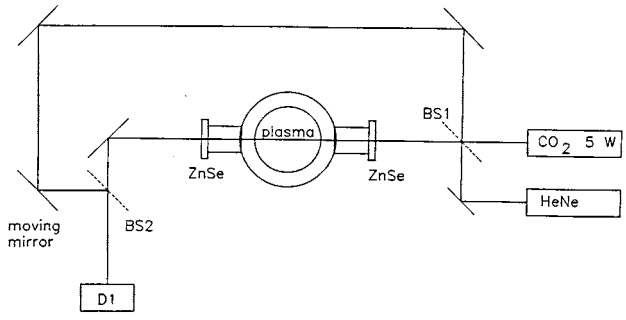

Figure 4: Schematic of the CO_2 interferometer.

Special attention has been paid to avoid attenuation of the probing laser beam in the plasma due to refraction or absorption. For this purpose we have measured the signal detected without the reference laser beam. For side-on measurements, no attenuation was observed during the first half of the magnetic field period. It is necessary to note that if the base pressure in the system, before filling the chamber with hydrogen, was high, we did observe a strong attenuation of the probing laser beam during the discharge. For the axial probing in the crowbar regime, because of the strong beam attenuation along the plasma axis, measurements could be performed only after 20 μs from the beginning of the discharge.

II.2. VUV and visible spectroscopy

A McPherson 225 Model vacuum monochromator (1 meter curvature concave grating, normal incidence, reciprocal linear dispersion 16.6 Å/mm)[5] was used for the end-on observation of the plasma line emission. Sodium salicylate scintillator and an EMI 9635B photomultiplier with bialkali photocathode were used for measurement of the plasma line emission intensity. A small 0.25 m visible monochromator was employed for side-on monitoring of the plasma continuum (bremmstrahlung) radiation in the wavelength regions of about 523 or 534 nm, free of line emission of hydrogen atoms, as well as atoms and ions of impurities (oxygen, nitrogen, carbon, silicon).

III. Results and discussion

III.1. Electron density evolution

To determine the evolution of the plasma density during the implosion phase of the discharge, interferometer measurements with side-on probing were performed. A typical interferometer signal obtained in the case of side-on probing is shown in the Fig. 5 together with the magnetic field time history. A low frequency of phase modulation has been used and before the main discharge the signal is determined only by the mirror movement. In the same figure the time evolution of the line plasma density obtained according to the procedure described above is also shown. It is possible to see that line plasma density increases with time and reaches $nl \sim 4.10^{15}$ cm^{-2} just after the moment of first maximum of the magnetic field. The filling pressure of H_2 for this case was about 0.7 mTorr, that corresponds to the density of hydrogen atoms after complete dissociation 4.10^{13} cm^{-3} and to the line atom density in the chamber $n_0 l_0 = 6.10^{14}$ cm^{-2}. Under the assumption of total ionization of hydrogen and conservation of the total number of electrons during implosion phase, one can estimate the average electron density at the moment of

maximum compression as (4 - 6).10^{15} cm^{-3} with the corresponding plasma diameter of about 1 cm.

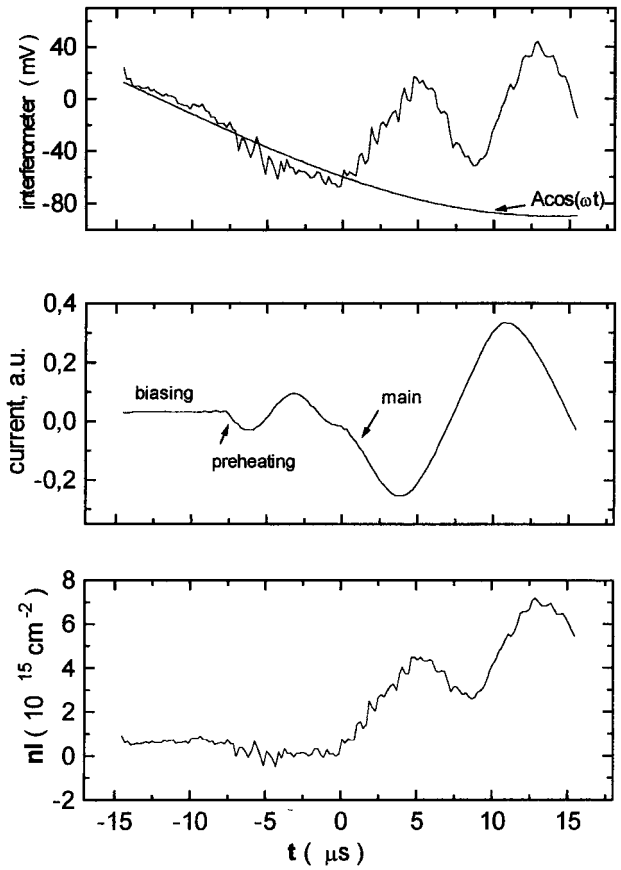

Figure 5: Experimental results for side-on measurements at the filling pressure of hydrogen 0.7 mTorr. Top: interference signal. Before the main discharge the signal is determined by the mirror movement. Middle: current in the theta-pinch coil. Bottom: time evolution of the line plasma density.

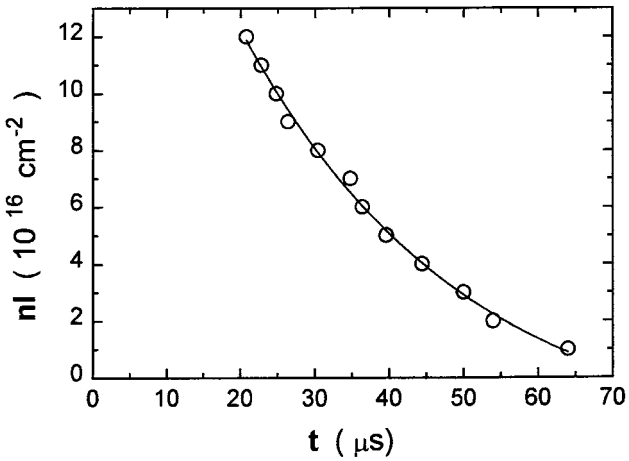

Figure 6: Time history of the line density of plasma measured along the axis in the regime with crowbar.

For the measurement of the plasma density evolution in the regime with crowbar, the longitudinal probing has been used (see Fig. 1). The results of the measurements are shown in Fig. 6. The plasma line density is decreasing from 1.2.10^{17} cm^{-2} to 4.10^{16} cm^{-2} during the period of 25 μs. For the plasma length of 60 cm the average plasma density at the moment 20 μs is equal to 2.10^{15} cm^{-3} at the axis of the discharge, and is in agreement with the measurements performed for the implosion phase of the discharge.

III.2. Study of the time history of impurity line emission

Temporal behavior of the line emission of oxygen and carbon ions for different ionization stages was studied. Hydrogen atomic lines were also observed in visible and VUV spectral regions. Strong emission of hydrogen lines typically was detected only in the initial phase of the discharge during an interval of about 1 μs. Some of the observed carbon and oxygen ionic lines are shown in the Table 1. The line threshold excitation energies and ionization energies are also presented in the Table 1.

Table 1. Wavelengths of the observed lines with the corresponding excitation and ionization energies for some carbon and oxygen ions.

Ion	Wavelength (A^0)	E_{exc} (eV)	E_{ion} (eV)
C III	2297	18	48
IV	1548	8	64
V	2271	304	392
O IV	2493	59	77
V	2781	72	114
VI	1032	12	138

Different temporal behavior of the line emission corresponding to the various ionization stages was observed with the increasing delay of the line peak emission for the increasing ion charge (see Figs. 7, 8). As it can be seen, the emission from the ions of the highest charges tends to peak near the maximum plasma compression.

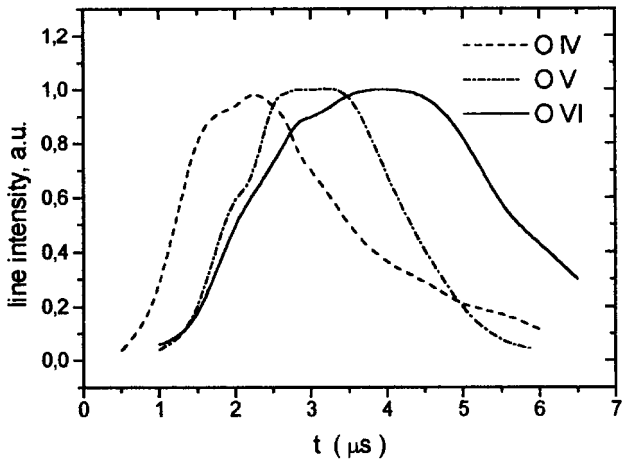

Figure 7: The time dependence of relative line intensities for O IV, O V and O VI ions in TC-1 theta-pinch plasma (intensities are normalized to the maximums).

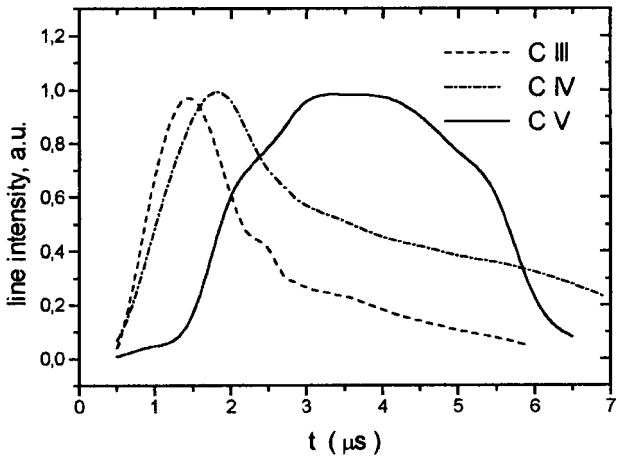

Figure 8: The time dependence of relative line intensities for C III, C IV and C V ions in TC-1 theta-pinch plasma (intensities are normalized to the maximums).

Time histories of ion line emission may be used for the evaluation of some plasma parameters[6,7]. Ions of the highest charges are localized in the hot plasma core, therefore their emission should be employed for characterization of the central part of plasma. For the lowest ion charges the emission from cold ends of plasma may be substantial (in the case of end-on observation), resulting in long lasting tails of the observed emission time history.

For the population of excited levels of impurity ions under theta-pinch discharge conditions the coronal model is usually valid. Then, for the end-on observation, the logarithmic derivative of optically thin line intensity P is given by[6]:

$$1/P(dP/dt) = (1/n_j)(dn_j/dt) + (1/n_e)(dn_e/dt) + \\ +(E_{exc}/kT_e - 1/2)(1/kT_e)(dkT_e/dt) + (1/L)(dL/dt) \quad (4)$$

where n_j is the total ion density of the j-ionization stage, n_e and T_e are the electron density and temperature, E_{exc} is the excitation energy threshold, L is the length of the plasma core. In the limit of negligible recombination, i.e. for the rapidly ionizing plasma[7],

$$dn_j/dt = n_e n_{j-1} I_{j-1} - n_e n_j I_j + (n_j/n_e)(dn_e/dt)\ , \quad (5)$$

where I_j is the rate coefficient for ionization and the last term is a source term, keeping the total concentration of the ions during compression (or expansion) phases of the discharge. For the quasi-stationary plasma, characterized by small variations of the plasma volume and density, the last term can be neglected.

Generally, both electron density and temperature variations affect strongly the line emission time history. However, during some interval at the maximum plasma compression the main plasma parameters may change only slightly. The length L of the plasma core is also known to vary slowly during the compression, and it will be considered further as a constant. Therefore, for the rapidly ionising plasma the late-time decay of the line intensity ($n_{j-1} \ll n_j$), observed during this particular period, from Eqs. (4,5) one can obtain:

$$1/P(dP/dt) = -n_e I_j \quad (6)$$

This gives us the possibility to evaluate ionization rate and, hence, electron temperature, if electron density is known. For the periods of substantial changes of electron parameters, the corresponding corrections should be done (the second and third terms in the right hand of the Eq.(4)). Note, that by choosing the lines with $E_{exc} \approx 1/2kT_e$, the contribution of the temperature dependent term can be made negligible.

Independent data on the electron density are available from two other diagnostics, used in the experiments for the same plasma conditions: ruby laser Thomson scattering and CO_2 - laser interferometry. From the interferometer measurements, which were performed with side-on plasma probing, the time evolution of the line plasma density $J(t) = \int n_e dl$ during the discharge is known (integration is made over the plasma

diameter). By use of Thomson scattering the local values of the electron density (and the electron temperature as well) can be measured. According to these measurements, the value of electron density in the center of the plasma near the maximum compression (4 μs after the initiating of the main discharge) was about $(5.7 \pm 0.5)x10^{15}$ cm^{-3} with the electron temperature of about 26 ± 4 eV. Under some assumptions, the time evolution of local electron density can be estimated by the use of these data. For simplicity, we will consider the electron density to be uniform within the plasma radius a , i.e. $n_e(r \leq a) = N_e$, and $n_e(r \geq a) = 0$.

The line plasma density $J(t)$ and the total number of electrons in the plasma $N_\Sigma(t)$ are related to the local density as follows:

$$J(t) \sim N_e(t)a(t) \ , \qquad (7)$$

$$N_\Sigma(t) \sim N_e(t)a^2(t) \ .$$

Then, for the case of pure hydrogen plasma, when the total number of electrons in the plasma core is constant (after the ionization is completed), the time dependence of local electron density can be expressed in terms of measured values:

$$N_e(t) = N_e(t_0)[J(t)/J(t_0)]^2 \ , \qquad (8)$$

where $N_e(t_0)$ the local density measured at the given time t_0. The time dependence of electron density, calculated by the use of Eq.(8) and the value of $N_e(t_0 = 4\mu s)$ $= 5.7x10^{15}$ cm^{-3}, is shown in the Fig. 9. To take into account the variation of the total number of electrons in the plasma during the discharge (due to the gradual ionization of impurities), the expression in the right-hand side of Eq.(8) should be multiplied by the additional factor $N_\Sigma(t_0)/N_\Sigma(t)$. It can be expected that, for the time interval under consideration (first period of plasma implosion), the percentage of impurities in plasma is relatively low. Thus, the effect of impurities on the $N_\Sigma(t)$ will not be considered here. Note, that for the case of a substantial impurity content, the calculations performed by use of Eq.(8), underestimate the electron density for the earliest phase of the discharge, when impurities are mainly in their lowest ionization stages (see Fig. 7, 8). It is worth noting that, in the case of discharge without crowbar, during the second period of implosion (after the plasma touching of the chamber walls), the impurity content in plasma was obviously much higher, resulting in the strong increasing of the ion line emission. Under these conditions, a substantial self-absorption of the impurity lines was observed in the centers of the spectral profiles. For the first period of implosion, no evidence of self-absorption was found.

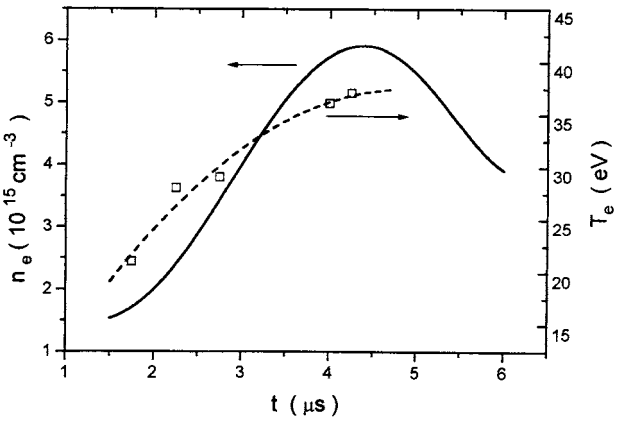

Figure 9: The time dependence of electron density, derived by use of Eq.(8) from the data of CO_2 laser interferometry (solid) and electron temperature, derived by use of Eq.(4) from the time history of impurity lines (dashed).

The data on time decay of ionic lines mainly were obtained for discharges without crowbar. For the OV and OVI lines, which peak near the maximum of compression, the time behavior was studied for the discharges both with and without crowbar, in order to check the effect of crowbar on the data obtained. Practically no difference was observed within the first 5-6μs, i.e., the effect of crowbar on plasma parameters was not substantial for this particular phase of discharge.

III.3. Electron temperature evolution

Further, by the use of the derived data on $N_e(t)$, the time evolution of collisional ionization rate and, hence, electron temperature during the discharge can be evaluated from the time decays of the different ionic lines. The temperature dependence of the electron impact ionization rates for different ions were calculated by use of the commonly employed semiempirical formula[7], assuming nearly all ions to be in their ground states:

$$I_j \cong 7.5 \times 10^{-8}(\eta_j/E_j)\{[\ln(40T_e/E_j)]^3 + 40\}[T_e^{1/2}/(E_j + 3T_e)\exp(-E_j/T_e), \quad (9)$$

where I_j is the rate coefficient for ionization (in cm^3/sec), h_j is the number of electrons and E_j is the ionization energy. The calculations of T_e were performed in a two-step iteration procedure: first, the $n_e(t)$-dependent corrections in Eq.(4) were taken into account, to obtain the first approximation for $T_e(t)$, and second, the $T_e(t)$-dependent corrections were introduced. The contribution of the second-step corrections was typically much less, than that of the first step. The results of calculations, performed in that way, are presented in the Table 2.

Table 2. Electron temperatures derived from the time decay of ionic lines (without and with corrections on electron density and temperature evolution, by use of Eqs. (6) and (4), respectively)

Ion	Time (μs)	T_e (eV)	
		Eq. (6)	Eq. (4)
C III	1.5-2.0	13	21
IV	2.0-2.5	18	28
O IV	2.5-3.0	20	29
V	3.5-4.5	33	36
VI	4.5-5.0	40	37

It can be seen, that the difference between values of T_e, obtained without and with corrections on electron density and temperature temporal variations, may be substantial (up to 50%) for the initial phase of the discharge, characterized by the rather fast changes of electron parameters. Since the electron density for the initial stage can be somewhat underestimated due to the effect of impurities (see above), the temperature values can be overestimated (with the effect being more pronounced for the very beginning of the implosion). For the period near the maximum compression (about 4 μs after initiating of the main discharge), when the electron density is changing slowly, the difference (Eq.(4) vs Eq.(6)) is less than 10%, i.e. within the experimental errors (33 and 36 eV). Typically, the accuracy of such measurements is estimated to be about 20%. So, the agreement with the data obtained by Thomson scattering for this moment (26 ± 4 eV), is quite satisfactory. Besides, Thomson scattering measurements were performed for the central part of the plasma core. However, the temperature distribution in a theta pinch plasma often has a dip in the center, with the temperature in the adjacent regions being 10-20% higher (see, for example, [6]). Therefore, since the radiation from plasma to VUV monochromator is collected from the larger area, the temperature derived from these measurements may be somewhat high. The time evolution of electron temperature, deduced from Eq.(4) , is also shown in the Fig. 9. It can be seen, that the rise of T_e during the compression is relatively slow, as compared with that of the density.

Results for C V line are not shown in the Table 2, since decay of this line emission occurs during the period of relatively fast decreasing of plasma density and, probably, temperature (later than 5 μs after the beginning of the discharge). Moreover, since the excitation energy for this line is rather high (see Table 1), $T_e(t)$-dependent corrections can be substantial. Under these conditions the accuracy of such measurements is not satisfactory. The use of this line time history may be helpful for the measurements of the higher plasma temperatures.

III.4. Ion temperature measurements

VUV spectroscopy was also employed for the measurements of ion temperatures T_i. The temperatures were derived from the Doppler-broadened widths (full width at half maximum) of ionic lines by use of expression $\Delta\lambda_D = 7.7 \times 10^{-5}\lambda(T_i\ [\mathrm{eV}]/\ M)^{1/2}$, where M

is the ion mass (in atomic units), λ is the line wavelength. The observed line broadening ($\Delta\lambda_{obs}$) is determined by the convolution of the Doppler-broadened line emission profile ($\Delta\lambda_D$) and the instrumental profile ($\Delta\lambda_{app}$). To derive the values of $\Delta\lambda_D$ from the observed line widths, the following relation was used: $(\Delta\lambda_D)^2 = (\Delta\lambda_{obs})^2 - (\Delta\lambda_{app})^2$. The data on the instrumental profile width for the monochromator employed in the experiments are presented in the Ref.5. The measurements of line profiles were performed with slits widths of $10^{-25}\mu$m by wavelength scanning in a large number of shots. Only line peak intensities were used. The following values of ion temperature have been deduced for the time interval near the maximum compression: $T_i = 70$ eV (O V line 2781 A^0, the first diffraction order, the line peaks at $t \approx 4\mu$s), and $T_i = 100$ eV (O VI line 1032 A^0, the second diffraction order, the line peaks at $t \approx 4.5\mu$s). The difference between T_i values obtained for different ions (at about the same time) could be interpreted partly in terms of the measurement accuracy. However, it should be noted that, in implosion plasmas, ions of higher charges can have higher temperature. The ion temperatures obtained exceed that for the electrons 2-3 times. A considerable difference between T_i and T_e is the intrinsic feature of the rapidly ionized theta-pinch plasmas. Indeed, under these conditions primarily the ions are heated. Moreover, electrons effectively lose their energy in inelastic collisions with atoms and ions during this phase of the discharge.

IV. Conclusions

In this work the results of the investigations of a fast theta-pinch discharge plasma by means of a number of optical diagnostics have been presented. The data on the temporal evolution of electron density have been obtained by use of CO_2 laser interferometry and Thomson scattering. The possibility to evaluate electron temperatures from the observed time history of line emission of impurity ions in VUV spectral region has been studied. A good agreement has been obtained with the results of Thomson scattering measurements. The ion temperature has been measured from the Doppler-broadened OV and OVI ion line profiles. It has been shown that the use of complementary information, obtained by means of different diagnostics, provides the opportunity to increase the accuracy and reliability of the data on fast plasma evolution.

Acknowledgments

This work was supported by Conselho Nacional de Desenvolvimento Científico e Tecnológico/RHAE, Conselho Nacional de Desenvolvimento Científico e Tecnológico - CNPq, Fundação de Amparo à Pesquisa do Estado de São Paulo - FAPESP, Financiadora de Estudos e Projetos - FINEP.

References

1. E. A. Aramaki, P. Porto, L. Berni, R.Y. Honda, M. Ueda, I. Doi and M. Machida, Nucl. Instr. Meth. Phys. Res., **A 280**, 597 (1989).
2. M. Tuszewski, Nuclear Fusion, **28**, 2033 (1988).
3. D. O. Campos, M. Machida, L. A. Berni, M.Yu. Kantor, S. A. Moshkalyov, S. V. Lebedev, in Proc. de 3^0 Encontro Bras. de Física dos Plasmas, 1995, Águas de Lindóia, SP, Brasil, p.90.
4. L. A. Berni, D. O. Campos, M. Machida, S. A. Moshkalyov, S. V. Lebedev, M. J. R. Monteiro and R. Zibordi, in Proc. de 3^0 Encontro Bras. de Física dos Plasmas, 1995, Águas de Lindóia, SP, Brasil, p.79.
5. S. A. Moshkalyov, M. Machida, S. V. Lebedev, D. O. Campos, Revista Bras. de Física Appl. Instr., **10**, 107 (1995).
6. P. Greve, M. Kato, H.-J. Kunze, R.S. Hornady, Phys.Rev., **A 24**, 429 (1981).
7. H.-J. Kunze, Phys.Rev., **A 3**, 937 (1971).